

Kelvin-Helmholtz instability in high-energy heavy-ion collisions

L.P. Csernai^{1,2,3}, D.D. Strottman^{2,3}, and Cs. Anderlik⁴

¹ *Department of Physics and Technology, University of Bergen, 5007, Bergen, Norway*

² *MTA Wigner Research Centre for Physics, 1525 Budapest, Pf. 49, Hungary*

³ *Frankfurt Institute for Advanced Studies, Johann Wolfgang Goethe University
Ruth-Moufang-Str. 1, 60438 Frankfurt am Main, Germany*

⁴ *Uni Computing, Thormøhlensgate 55, N-5008 Bergen, Norway*

(Dated: April 12, 2012)

The dynamical development of collective flow is studied in a (3+1)D fluid dynamical model, with globally symmetric, peripheral initial conditions, which take into account the shear flow caused by the forward motion on the projectile side and the backward motion on the target side. While at $\sqrt{s_{NN}} = 2.76$ A TeV semi-peripheral Pb+Pb collisions the earlier predicted rotation effect is visible, at more peripheral collisions, with high resolution and low numerical viscosity the initial development of a Kelvin-Helmholtz instability is observed, which alters the flow pattern considerably. This effect provides a precision tool for studying the low viscosity of Quark-gluon Plasma.

PACS numbers: 24.85.+p, 24.60.Ky, 25.75.-q, 25.75.Nq

I. INTRODUCTION

Global collective observables are becoming the most essential in ultra-relativistic heavy ion reactions [1]. When we want to extract information from experiments, both on the equation of state (EoS) and the transport properties of matter [2, 3], we have to invoke a realistic description with a fully (3+1)D dynamical evolution at all stages of the reaction, including the initial state.

It is important to note that the phase transition to quark-gluon plasma (QGP) and consequent fluctuations may enhance the collective behavior of the system [4]. For the fluid dynamical (FD) initial state we must have a system that is close to local equilibrium; thus, at high energies the transition to QGP has to happen earlier than the formation of the locally equilibrated initial state.

The (3+1)D, relativistic FD model we use to describe energetic heavy ion reactions is well established and describes the measured collective flow reliably [5, 6]. We use the Particle in Cell (PIC) method in which an Eulerian grid contains a very large number of Lagrangian marker particles that move with the matter. This method enables us to follow the motion of the fluid with good precision. At Large Hadron Collider (LHC) energies in these calculations we observed a significant rotation of the QGP fluid in peripheral collisions, which leads to observable consequences [6].

Our detailed studies indicate the development of an interesting phenomenon, namely the beginning of a physical instability. In peripheral collisions, in the transverse, $[y, z]$ plane a non-sinusoidal instability starts to develop. We can visualize this by coloring the markers in the projectile (upper) side blue and the target (lower) side red. Initially the dividing surface is a plane. As time proceeds, the markers (which indicate the location of conserved baryon charge) move, and the dividing surface becomes a wave, which resembles the start of a Kelvin-Helmholtz (KH) instability as shown in Fig. 1 in the $[x, z]$, reaction plane, *i.e.*, $|y| \leq 1$ cells ($|y| \leq 0.7$ fm).

Initially, at 1.5 and 3.0 fm/c, we can see two shorter wavelength KH instabilities, which then dissolve and are fed into a longer wavelength instability.

The non-sinusoidal behaviour of the instability at later times is not obvious as the development of instability and the spherical expansion compete with each other.

The density of the central zone decreases rapidly so that the matter “freezes out” and the fluid dynamical description breaks down. As a consequence we do not see the vorticity sheet rolling up as in a fully fledged KH instability. In more central collisions the dividing surface nearly remains a plane. The usual reason for the KH instability is a “shear flow”, where in a fluid layer there is a large velocity gradient. Thus, the origin and the energy source of this phenomenon is in the initial configuration and the initial velocity distribution, which are correctly represented in our initial state model [7].

In our computational fluid dynamics (CFD) calculation the initial state model –based on longitudinally expanding flux tubes or *streaks* [7]– is used [5, 6]. In non-central collisions only a part of the original nuclei interact. These are in the participant zone where the streaks develop. Spectator nucleons on the two sides are not participating in the reaction.

The participant streaks are formed by the color charges arising from the projectile and target nuclei after these have penetrated through each other. The chromo-electric field, characterized by the *string tension*, slows down the expansion of the ends of the streaks. Our FD initial state is a configuration where the matter is stopped within each streak, while streaks expand independently of each other. Thus, this model is applicable streak by streak and the momentum of the streaks varies, especially for the peripheral streaks where the asymmetry between the projectile and target contribution to the participant matter is the biggest. So, the streaks at the projectile and target sides move in the beam (z) direction with substantial velocity difference. This generates the shear flow configuration.

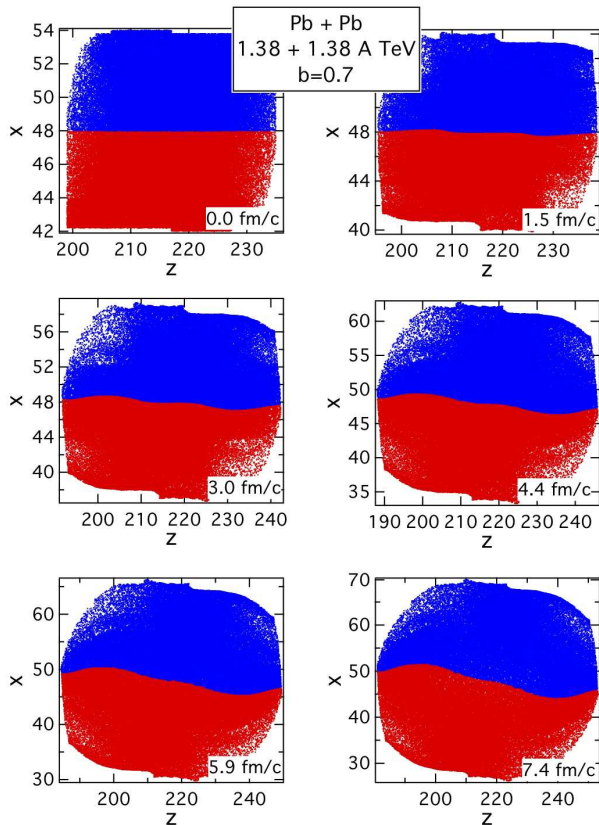


FIG. 1: (color online) Growth of the initial stage of Kelvin-Helmholtz instability in a 1.38A + 1.38A TeV peripheral, $b = 0.7b_{\text{max}}$, Pb+Pb collision in a relativistic CFD simulation using the PIC-method. We see the positions of the marker particles (Lagrangian markers with fixed baryon number content) in the reaction plane. The calculation cells are $dx = dy = dz = 0.4375 \text{ fm}$ and the time-step is $0.04233 \text{ fm}/c$. The number of randomly placed marker particles in each fluid cell is 8^3 . The axis-labels indicate the cell numbers in the x and z (beam) direction. The initial development of a KH type instability is visible from $t = 1.5$ up to $t = 7.41 \text{ fm}/c$ corresponding from 35 to 175 calculation time steps).

The aspect ratio of matter in the reaction plane ($[x, z]$ -plane) becomes more elongated with increasing impact parameter, b , as the height of the participant profile, L , becomes smaller, $L = (2R - b)$, for nuclei of radius R , and the streaks are becoming longer due to the smaller effective string tension [7]. Thus, the aspect ratio for $b = 0.5b_{\text{max}}$ (where $b_{\text{max}} = 2R$) is $[1 : 1.5]$, while for $b = 0.7b_{\text{max}}$ it is $[1 : 3]$. Of course this aspect ratio depends on the initial state model, and some of these do not take into account the longitudinal expansion before thermalization, and even less the dependence of the expansion on the effective string tension.

In a heavy ion reaction the projectile edge of the participant domain moves almost with the velocity of the projectile, u , while the target side moves with the target velocity, $-u$. At high energy this difference provides considerable shear in the velocity fields. At the same time in the initial state model [7] the initial transverse velocity

is zero for all fluid elements. A low $[x : z]$ -profile makes it possible to develop a typical shear-flow configuration and thus, there may be a possibility to form the initial stages of a KH instability.

II. PHYSICAL CONSIDERATIONS

A. Growth of the KH instability

The growth of a small initial KH instability in an idealized shear-flow configuration can be described in a rather simple way. From ref. [8] sect. 3 it follows that the shear flow starting from a small sinusoidal perturbation in incompressible and inviscid flow, the perturbation will grow exponentially, $\propto \exp(st)$, ([8] 3.15), where t is the time and s is proportional to the wave number k ,

$$s = kV$$

([8] 3.28) where $\pm V$ is the characteristic velocity of the upper/lower sheets which is somewhat less than the projectile or target velocity.

Thus, the largest k or shortest wavelength will grow fastest. Also, increasing the beam energy (i.e. increasing V) will also lead to increased development of turbulence!

For a Pb+Pb reaction, $R = 7 \text{ fm}$, $b_{\text{max}} = 14 \text{ fm}$, we study the impact parameters $b = 0.5$ or $0.7b_{\text{max}}$. For these collisions the typical transverse size of the initial shear flow is

$$L = (2R - b) = 7.0 \text{ or } 4.2 \text{ fm}.$$

The typical calculation cell size is $dx = dy = dz = 0.35 \text{ fm}$. The beam directed, longitudinal length of the initial state is

$$l_z = 10.5 \text{ or } 13.1 \text{ fm}, \quad (1)$$

and the minimal wave number is

$$k = 2\pi/l_z = 0.598 \text{ or } 0.479 \text{ fm}^{-1}$$

respectively.

For the scaling analysis of instabilities we need the dimensionless numbers constructed from the typical length, L , and speed, V . The Reynolds number is $Re = VL/\nu$, where ν is the kinematic viscosity. So, for a peripheral heavy ion collision with impact parameter b , the characteristic length is L and V is the velocity of the top/bottom layer, $V = |u|$. In exactly central collisions $u = 0$, while with increasing impact parameter, $u = \pm 0.26, 0.34, 0.36, 0.39, 0.43, 0.42, 0.39 c$ for $b = 0.1, 0.2, 0.3, 0.4, 0.5, 0.6, 0.7 b_{\text{max}}$, respectively. Notice that due to the geometry and the minimal string diameter of 1 fm , the increase of this velocity does not reach the beam velocity, so for typical peripheral collisions $V = |u| \approx 0.4c$.

In the simplest incompressible and inviscid flow approximation the amplitude of of the starting turbulence

would double in 2.90 or 3.62 fm/c for $b = 0.5$ or $0.7b_{\text{max}}$. The growth of instability is very fast in this approximation and it increases with the beam energy (beam velocity) and with the wave number. The typical reaction time in a heavy ion collision exceeds the time needed to double the amplitude of an initial instability.

At the same time we also observe that at smaller impact parameters the development of an instability is not seen in our calculations, see Fig. 2. Thus, we have to conclude that the role of viscosity is decisive as a large viscosity will decrease this growth rate and may eliminate the possibility of the KH instability.

B. Formation of critical length KH instability

While perturbations with larger wave number (shorter wavelengths) may grow faster, there is a critical minimal wavelength beyond which the perturbation is stable and able to grow. Smaller wavelength perturbations tend to decay into random thermal fluctuations. This situation is analogous to the phase transition dynamics via homogeneous nucleation where the formation of critical size bubbles or droplets is required to start the phase transition [4].

This aspect of turbulence formation was first discussed by Kolmogorov [9] for flow in the “inertial range” where the effects of viscosity are still negligible. These considerations are applicable until the viscosity does not have a significant effect on the formation of vortices. The minimal stable wavelength for a starting instability is given by the Kolmogorov length scale, which is the smallest scale of turbulence. Dominant and increasing viscosity results in increasing critical vortex size, λ_{Kol} . Smaller perturbations are unstable.

The average rate of energy dissipation, ϵ , per unit mass and unit time, is associated with the decay of an eddy of size l and characteristic speed, v_l into two smaller ones, in time $t_l = l/v_l$. It follows then that $\epsilon \sim v_l^2/t_l = v_l^3/l$. The decay (or formation) time of the small size eddy, t_l , can be compared to the viscous diffusion time of a perturbation of size l , which is $t_l^{\text{dis.}} = l^2/\nu$. Equating the two estimated characteristic times provides the minimal, Kolmogorov length, λ_{Kol} :

$$\lambda_{\text{Kol}} = [\nu^3/\epsilon]^{1/4}. \quad (2)$$

Here ν is the kinematic viscosity of the fluid, $\nu = \eta/\rho = \eta/(nm_B)$, where η is the shear viscosity, ρ is the mass density, n is the baryon charge density and m_B is the characteristic mass falling on unit net baryon charge in QGP.

Even if the average rate of energy dissipation, ϵ , is proportional to the viscosity, this dependence is linear, so the critical vortex size is still increasing with increasing viscosity. The key question is: can a critical size vortex be formed in a heavy ion collision? Lower viscosity and higher energy or energy dissipation may enable the formation of a critical size or larger vortex.

Kolmogorov’s theory also provides an energy distribution spectrum for small vortices or whirls in nearly perfect fluids. The energy density spectrum in terms of the scale of the vortices, λ , is proportional to $\lambda^{-1/3}$, i.e., it is lower for larger vortices. Large vortices may generate smaller ones, until we reach the viscous limit, λ_{Kol} , where the vortices are becoming just thermal fluctuations.

In non-relativistic flow the mass flow is identical with the flow of massive particles while the flow energy and the thermal energy are negligible compared to the rest mass of the fluid. At ultra-relativistic energies this is not the case and the separation of flow (inertial) energy and the random thermal energy is not a trivial question. In order to follow the classical concepts turbulence and its development we will follow Eckart’s definition of flow velocity, where flow is bound to the conserved net baryon charge and we will assume that the flow of the average of all quarks can be characterized by this velocity. The observed constituent quark number scaling of collective flow observables for different hadrons supports this approach.

We focus on the description of the initial stages of the development of turbulent instability in the central zones of the collision at a period just after the formation of the locally equilibrated FD initial state. We will estimate the corresponding collective mass of the partonic matter in QGP per unit baryon charge, m_B , at this stage of the reaction. Before the collision at the LHC each nucleon has 1.38 TeV energy. Local equilibration is reached when, for $b = 0.7b_{\text{max}}$ impact parameter, in the first 3 fm/c time after initial equilibration the average temperature is $T \approx 400 \div 600$ MeV, the average entropy density is $s \approx 150 \div 440$ fm $^{-3}$, the average baryon charge density is $n = 0.1 \div 0.16$ fm $^{-3}$ and the average internal energy is $T(s/n) = T\sigma = e/n \approx 1.1 \div 1.3$ TeV/nucleon, where σ is the specific entropy per unit baryon charge. At the initial stages of QGP flow the remaining energy is shared between collective flow energy and particle mass of all constituents, plus a smaller amount may go to pre-equilibrium emission of high energy particles. Thus, the effective mass can be estimated as $m_B \approx 100$ GeV per unit baryon charge.

By late stages of the reaction the kinetic energy of the flow increases substantially, while the dissipation increases the thermal energy by about 4 ÷ 6% [10]. The total hadron multiplicity increases by about an order of magnitude, so the effective mass per net baryon charge is of the order of $m_B \approx 10$ GeV. We are interested in the case of initial QGP in local equilibrium when the KH instability could start.

The shear viscosity is temperature dependent with a sharp minimum at the critical point of the phase transition between hadronic matter and QGP [3], and reaching unity at the initial hot, compressed QGP at about $4T_c$:

$$\frac{\eta}{s} \approx 1 \div 2 \hbar,$$

which for the initial QGP gives

$$\eta = s\hbar \approx 30 \div 158 \text{ GeV}/(\text{fm}^2 \text{ c}),$$

and about 10 times less for the minimal viscosity. Considering that the initial effective mass density may vary between, $\rho = nm_B \approx 10 \div 16 \text{ GeV}/(\text{fm}^3 \text{ c}^2)$, the corresponding kinematic viscosity is

$$\nu = \frac{\eta}{\rho} = 2.5 \div 16 \text{ fm c},$$

and about 10 times less for the minimal viscosity.

The corresponding Reynolds number is $Re = 0.3 - 1$ (for “ $\eta/s = 1$ ”), and if we choose the minimal viscosity (“ $\eta/s = 0.1$ ”), then $Re = 3 - 10$. These are small Re values for turbulent flow in general, but the KH instability can also appear for small Re [8].

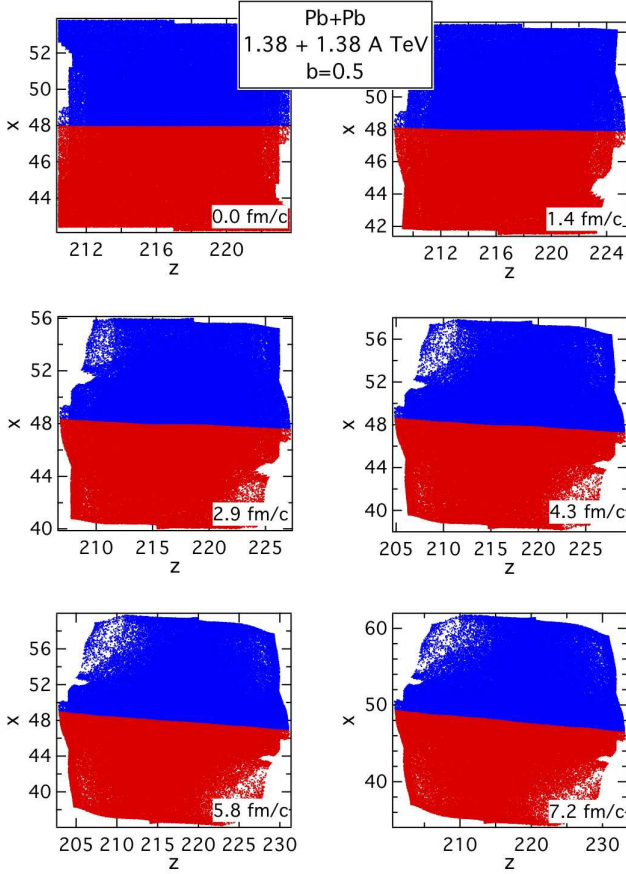


FIG. 2: (color online) Time evolution of the flow in 1.38A + 1.38A TeV peripheral, $b = 0.5b_{\text{max}}$ Pb+Pb collision. The calculation cells are $dx = dy = dz = 0.585 \text{ fm}$ and the time-step is 0.08466 fm/c . The number of randomly placed marker particles in each fluid cell is 8^3 . In contrast to Fig. 1 the KH instability does not develop during the initial $\sim 8 \text{ fm/c}$ time, due to the increased numerical viscosity and the similar length and height of the initial state. Thus the sides of the fluid provide a stiffer formation and the system rather rotates as a solid body, instead of forming an expanding turbulent, rotating shell. Due to angular momentum conservation the rotation slows down as the system expands.

If we have a perfect fluid the flow is adiabatic, there is no dissipation, so $\lambda_{\text{Kol}} \sim (0/0)!$ The specific dissipated

flow energy to heat is

$$\epsilon = \dot{e}/\rho \propto T\dot{\sigma}/\rho \propto \nu, \quad (3)$$

where the dot indicates the proper-time derivative, $\dot{e} \equiv \partial_t e$ is the change of energy density with time, T is the temperature and $\dot{\sigma}$ is the proper time derivative of the specific entropy density, σ . Thus if $\nu \rightarrow 0$ then $\lambda_{\text{Kol}} \rightarrow 0$. So, the minimal size will grow from zero if the viscosity grows. With finite viscosity one can have a large minimal size, so that the turbulence can not develop within the given length of the system. As in the final expanding stages of the QGP fluid the viscosity increases [3], the minimal eddy size, λ_{Kol} , will be larger, so initial smaller length instabilities will disappear.

A good example for the formation of a minimal size eddy can be observed in a two-component Fermi-gas (e.g. Li-6), which forms a super-fluid at low temperatures in a rotating magnetic trap [11]. If we reach a limiting rotation frequency, a small eddy may develop in the central region of the cylindrical trap when the energy of a small critical size eddy will be sufficient to balance the viscous dissipation, and this eddy may become stable. One also needs a given viscosity or scattering length to form this eddy in the middle, thus the eddy first appears at a given finite scattering length! See Fig. 14 of ref. [11]a. The minimal KH instability has similar minimal size behaviour, although the shear-flow geometry is different; one needs a minimal torque from the boundary condition and a minimal viscosity to form a critical eddy.

Let us make a very simplified estimate for the size of the smallest possible eddy in a heavy ion collision. For finite shear viscosity the energy dissipation per unit mass and unit time, $\epsilon = \dot{e}/\rho$, depends on the viscosity as well as the flow pattern. The characteristic shear V/L depends on the impact parameter, so that $(V/L)^2 = 0.0038 \div 0.0086 (\text{c}/\text{fm})^2$ for $b = 0.5 \div 0.7b_{\text{max}}$, respectively. For the ideal shear flow the dissipated energy with the minimal viscosity (“ $\eta/s = 0.1$ ”) is (see [12] sect. 16 or [13] sect. 1.6):

$$\begin{aligned} \epsilon &\approx \eta \left(\frac{V}{L} \right)^2 = \\ &= \begin{cases} 11 \div 26 \text{ MeV c}/\text{fm}^4 & \text{for } b = 0.5b_{\text{max}} \\ 61 \div 138 \text{ MeV c}/\text{fm}^4 & \text{for } b = 0.7b_{\text{max}}. \end{cases} \end{aligned} \quad (4)$$

Then the energy dissipation, with an estimated average unit mass density of $\rho = 13 \text{ GeV}/(\text{fm}^3 \text{ c}^2)$, gives the rate of energy dissipation $\epsilon = \dot{e}/\rho$ and thus the Kolmogorov length is

$$\lambda_{\text{Kol}} = \begin{cases} 2.1 \div 5.4 \text{ fm} & \text{for } b = 0.5b_{\text{max}} \\ 1.4 \div 3.6 \text{ fm} & \text{for } b = 0.7b_{\text{max}} \end{cases} \quad (5)$$

In peripheral heavy ion collisions the KH instability can develop only if

$$l_z > \lambda_{\text{Kol}}. \quad (6)$$

Thus, comparing the above values of the Kolmogorov length scale to the length of the initial state in the beam direction, eq. (1), we can see that at $b = 0.7b_{\text{max}}$ we may have a possibility to initiate a KH type instability in a heavy ion collision, while at smaller impact parameters this possibility is marginal. This is enhanced by the fact that viscosity and the Kolmogorov length increases with expansion, so the time-slot where the KH instability may develop is reduced for more central collisions.

Based on eqs. (2,4) we see that in our situation the Kolmogorov length is proportional with the square of viscosity, $\lambda_{\text{Kol}} \propto \eta^2$, so if the viscosity doubles, the Kolmogorov length, eq. (5), increases by a factor of four, so it can reach 20 fm, which exceeds the longitudinal system size, and hinders the development of the KH instability up to about 8 fm/c. This is illustrated in Fig. 2 with the increased numerical viscosity. The change of marker particle resolution does not influence the disappearance of the KH instability.

The characteristic geometry of the KH instability (approximately two planes close to each other) require that $L < R$ or $b \geq R$, and so b may vary in the interval between $0.5b_{\text{max}}$ and $0.8b_{\text{max}}$ where $b_{\text{max}} = 2R$. At larger impact parameters L becomes too small and the general applicability of a continuum approach becomes questionable. So, this parameter cannot vary too much, and condition (6) requires to have a viscosity smaller than a limiting value,

$$\nu_c \simeq 5 \text{ fm } c,$$

which is satisfied by the low viscosity QGP, even at higher than critical temperatures.

III. FLUID DYNAMICAL MODEL PREDICTIONS

We have performed CFD simulations with the PIC solution method [5, 6] where the equations of relativistic FD were solved for a perfect quark-gluon fluid. At the same time the numerical method, due to the finite grid resolution, led to dissipation and thus to entropy production, which has been analysed [10]. From the entropy production we could determine the corresponding “numerical viscosity”, and this was approximately the same as the estimated, low viscosity of the quark gluon plasma. To avoid double counting, *i.e.*, over counting of viscous dissipation, we did not add additional viscous terms to our CFD model simulations ¹.

Our numerical model predictions confirm the previously presented physical conclusions, and these show a developing instability which is visible at $b = 0.7b_{\text{max}}$ (Fig. 1), but at the smaller impact parameter the KH instability is weak and does not change with increasing resolution, see Fig. 3. Increasing the resolution by 67% at $b = 0.7b_{\text{max}}$ increases the amplitude of the KH instability wave by 57%. The final KH instability amplitude (1.1 fm) is 6% of the final profile height (and 16% of the initial one).

In the case of heavy ion collisions the special geometry, *i.e.*, the shape of the participant zone, is also hindering the development of the instability because the more extended side-walls at smaller impact parameters have a stabilising effect against the KH instability.

We can observe in our calculations that the initial sinusoidal wave shape will become asymmetric in standard plane shear flow (see [8] Fig. 3.3 or [14] Fig. 2), especially at points of accumulating vorticity.

The PIC method has a particular advantage in studying the KH instability. The numerical viscosity is set by choosing a calculation grid size, which provides the estimated small dissipation of the viscous QGP fluid. At the same time the PIC method has a large number of marker particles in each Eulerian fluid cell. Their number can vary, and can be orders of magnitude higher than the number of Eulerian fluid cells forming the fixed calculation grid. Thus the motion of the marker-particles provides a fine resolution and can follow the dynamics of the flow more accurately. In this method the marker particles provide an accurate tracing of the initial development of the KH instability.

In connection with our CFD solution one has to mention that the *numerical viscosity* of our model calculation is small, $\eta/s = 0.1$, based on the small Eulerian cells. In addition the number of initial marker particles per normal density cell was changed from $3^3 = 27$ to $9^3 = 729$ so that the higher Lagrangian resolution allows for a more accurate description of the instability.

In case of heavy ion reactions the flow is not stationary and the shear flow geometry is only present in the initial state. Later, due to the large pressure of QGP the plasma explodes and expands radially in a way that the final flow pattern at freeze out is close to spherical albeit somewhat elongated longitudinally and in the reaction plane ($\pm x$ -direction) due to the dominant elliptic flow.

¹ In numerical, CFD simulations of instability, it is important to study the dissipative effects of both the numerical viscosity and the physical viscosity. A finite grid resolution in the CFD solutions leads to the absorption of the shorter wavelength and high frequency fluctuations, and the energy of these fluctuations is converted into heat. There exist solution methods, with finite

computational grid resolution, which enforce entropy conservation for perfect fluids. These solutions then appear to be perfect adiabatic fluid flow solutions. However, this is misleading, such a numerical solution still absorbs high frequency small wavelength perturbations, while the energy of these is converted into large wavelength fluctuations. Thus, such methods may result in misleading results.

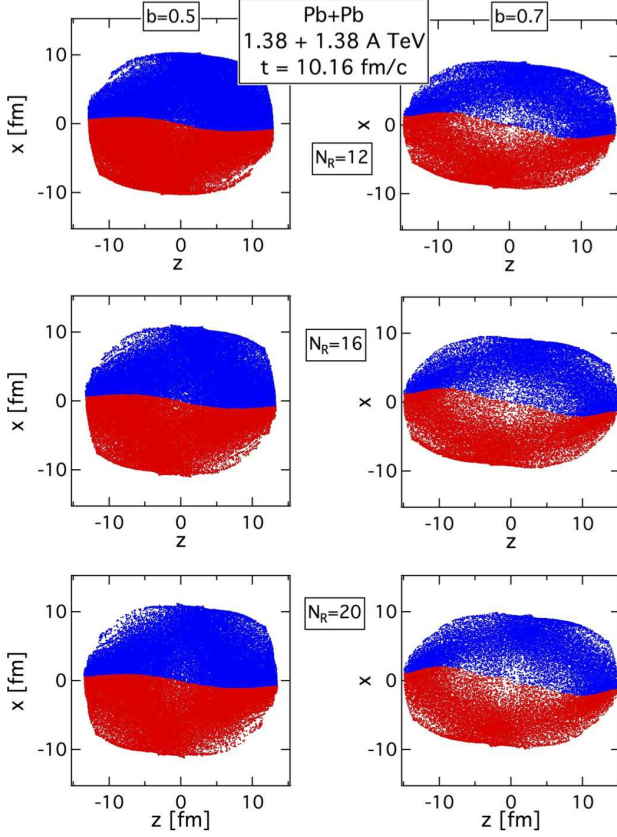


FIG. 3: (color online) Comparison of the flow pattern in the reaction plane in 1.38A + 1.38A TeV peripheral, Pb+Pb collisions at two impact parameters: $b = 0.5b_{\text{max}}$ (left column) and $b = 0.7b_{\text{max}}$ (right column), at a late stage of 10.16 fm/c (240 time-steps). By this time an instability wave is also noticeable at $b = 0.5b_{\text{max}}$. The resolution increases from the top to the bottom as $dx = 0.585, 0.4375, 0.35$ fm (i.e. $N_R = R_{\text{Pb}}/dx = 12, 16, 20$). The number of marker particles were $8^3, 6^3$ and 5^3 for these resolutions, so that each of the marker particles carried about the same amount of baryon charge: $5.61, 5.61, 4.97 \times 10^{-5}$. For the impact parameter $b = 0.5b_{\text{max}}$ independently of the resolution and numerical viscosity the rotation of the dividing plane is 2 degrees, and the amplitude of the KH instability wave is not bigger than 0.35 fm. For the impact parameter $b = 0.7b_{\text{max}}$ the rotation of the dividing plane is 3.75 degrees for all resolutions, but the amplitude of the KH instability wave is increasing with increasing resolution (decreasing numerical viscosity) as: 0.7, 0.9 and 1.1 fm.

A. CFD Results

In heavy ion reactions the radial expansion modifies the dynamics of the development of the KH instability, but in case of low viscosity this is a strong instability and its initial signs can be clearly recognized in CFD calculations if both the viscosity and the numerical viscosity are sufficiently small. Looking at Fig. 1 initially at $N_{\text{cyc}}=0$, the fluctuation is not visible, although the randomly placed markers include a possibility for fluctu-

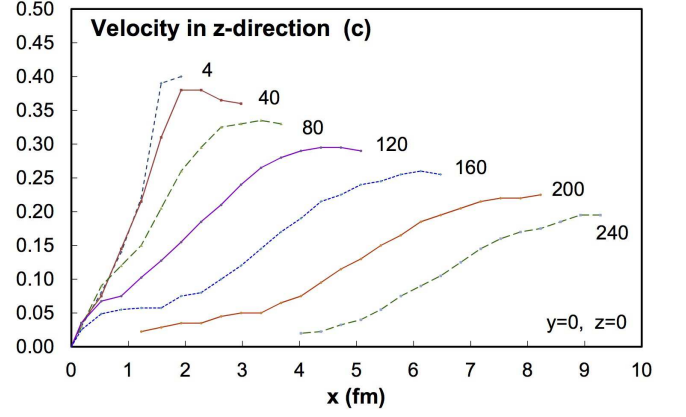


FIG. 4: (color online) The velocity profile in the beam direction as a function of the x -coordinate, at different times, 4, 40, 80, 120, 160, 200 and 240 time-steps of 0.04233 fm/c for $b = 0.7b_{\text{max}}$, cell size $dx = 0.35$ fm and 7^3 marker particles per fluid cell. The velocity is plotted in the reaction plane, (at $y = 0$ and $z = 0$), and it is antisymmetric in the $\pm x$ -direction, but only the upper $x > 0$ half of the reaction plane is plotted. In the CFD calculation the mirror symmetry is exact.

ations (the length of the system is 35 cells). At 1.5 fm/c ($N_{\text{cyc}}=35$), there appear two semi-sinusoidal waves. The length of the system is 45 cells. The amplitude of turbulence is ≈ 1 cell. At 3.0 fm/c ($N_{\text{cyc}}=70$) the length of the system is ≈ 50 cells. The central perturbation of 15 cell wavelength weakening while the outside part grows. The amplitude of turbulence is ≈ 3 cells. At 4.4 fm/c ($N_{\text{cyc}}=105$) the middle middle perturbation wave is weakening further, and the amplitude of the turbulence is ≈ 4 cells. By 5.9 - 7.4 fm/c ($N_{\text{cyc}}=140 \div 175$) the middle, short wavelength perturbation is hardly visible. The amplitude of the turbulence has reached $6 \div 10$ cells.

Due to the fact that the radial expansion and the shear flow are superimposed upon each other the growth rate and the wave shape of the developing turbulence are not identifiable fully as in (quasi-) stationary flow. The initial shorter wavelength perturbations become unstable and disappear, while the longest one grows due to the radial expansion. This can be attributed to the fact that the Kolmogorov minimal size is increasing faster than the expansion, thus the short perturbations are becoming unstable while the largest one survives.

The phenomenon enables us to draw some quantitative consequences from the physical viscosity of QGP on qualitative differences in the flow pattern. The smaller central perturbation which disappears during expansion is not detectable. The larger one develops if the available length of the system exceeds the Kolmogorov length scale. Then the shortest of these possible perturbations will grow fastest and will lead to enhanced and observable “rotation”. Increased beam energy leads to increasing V , which leads to an exponential increase in the growth of the instability, much more than just the linearly increased angular momentum would cause!

As the estimates of the previous section indicate, the development of the KH instability is critically dependent on the flow configuration, and just as the numerical estimates for λ_{Kol} indicate the CFD results for impact parameter $b = 0.5b_{\text{max}}$ also show that the KH instability is weak and it does not develop with increasing resolution for more central collisions, see Fig. 2.

The dynamics in the CFD model indicates that the KH instability may start to develop in ultra-relativistic heavy ion collisions. The numerical viscosity in the calculation is about the same as the conjectured minimal viscosity [2] as discussed in ref. [10].

The analysis in the previous section assumed an initial viscosity based on ref. [3] which was around the minimal viscosity and it was sufficient to develop the critical size KH instability. An order of magnitude larger viscosity would not be able to create a sufficiently small initial perturbation.

B. Instability estimates for viscous fluids

In shear flow one of the necessary conditions for the start a KH instability is that there should be an inflection point in the basic velocity profile $u_z(x)$, or in other words $u_z''(x)$ must change sign at least once [8] Sect. 8. The initial condition [7] and the subsequent flow satisfy this requirement.

As Fig. 4 shows, at time-step 4 and 40 the condition is satisfied in the center ($x = 0$), later at steps 80, 120 and 160 a second wave develops, however the distance of the nodes is less than λ_{Kol} , so considering the viscous limits these secondary waves are not realizable physically. For a single wave of KH instability the situation is established, and persists up to time-step 120. By time-step 160 the central density drops considerably and apart from short length fluctuations the required condition is not satisfied.

This is due to the fact that in the discussed heavy ion collision, we do not have a stationary boundary condition, and the spherical expansion competes with the growth of KH instability. At later stages, time-step 160 and later, the growth speed, kV decreases, as both the velocity and the wave number decrease, while the expansion speed is increasing. Thus at time-step 160 the flow goes over to a combined approximately radial expansion and rotation. On the other hand by this time the system is close to freeze out and hadronization. At this time the matter is dilute and weakly interacting, so the local fluid dynamical equilibrium cannot be maintained and the FD description will not be applicable.

The central zones at late stages have low density and low pressure, which resembles a cavitation bubble in the QGP liquid and this bubble will contain the condensed hadrons. Due to the expansion the bubble will not recollapse as usual in cavitation phenomena in classical fluid flow; instead the surrounding QGP fluid will break up into peaces and will also hadronize and freeze out simultaneously.

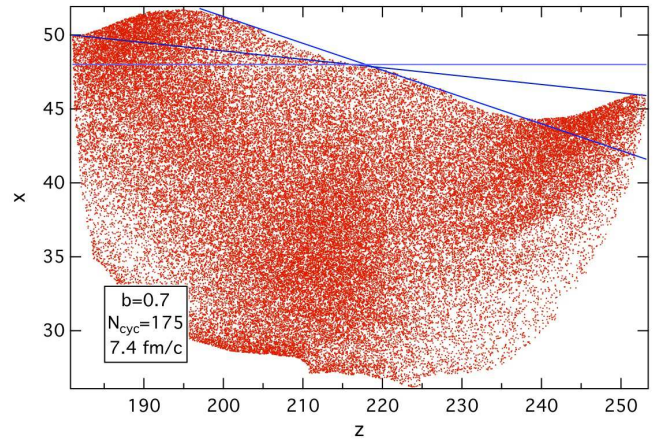


FIG. 5: (color online) The detailed view of the marker particle positions in the lower half of the initial state markers after 175 time-steps. A 1.38A + 1.38A TeV energy Pb+Pb peripheral collision is shown, at $b = 0.7 b_{\text{max}}$ impact parameter with $7^3 = 343$ markers per initial, normal density fluid cell resolution. The lines across the collision center point indicate the initial dividing axis, the change of this axis due to rotation and the additional change of rotation arising from the start-up of a Kelvin-Helmholtz type of instability. This additional effect more than doubles the rotation. In this calculation the cell size is $dx = dy = dz = 0.35$ fm, with a total number of 1814814 marker particles.

IV. CONCLUSIONS

Based on theoretical estimates and on CFD model calculations, one should explore the possibility at LHC energies of a KH instability developing in peripheral, $b = 0.6 - 0.8b_{\text{max}}$ Pb+Pb collisions. The formation of the instability may take place up to about 5 fm/c, beyond which the radial expansion becomes dominant although the system still rotates.

The KH instability is rather sensitive to the value of viscosity, so it is a perfect tool to measure the viscosity of QGP. The rotation of the weak anti-flow peak to forward angles was predicted earlier [6]. The rotation of the v_1 -peak to forward angles depends sensitively on the balance between the speed of radial expansion/explosion and the initial angular momentum (which increases with increasing beam energy). If the radial expansion is stronger than estimated [6] then the peak may remain an "antiflow" peak and the KH instability would destructively interfere with this peak. If the peak has rotated to forward angles as predicted in [6] and used also in these calculations, the KH instability increases the rotation and it converts a larger part of beam energy into rotation than it would happen in a simple solid body type of rotation. See Fig. 5.

At cycle 160 ($t = 6.77$ fm/c) using the method of ref. [6] primary $v_1(y)$ values for massless pions were evaluated for two different impact parameters, $b = 0.5, 0.7b_{\text{max}}$, and for different grid resolutions. The number of marker par-

ticles were chosen so that the number of marker particles per baryon charge was about the same, 20120 for cell size $dx = 0.35$ fm and 17825 for cell size $dx = 0.585$ fm. For the Pb+Pb reaction at $b = 0.5b_{\text{max}}$ and $dx = 0.585$ fm resolution the directed flow peak was at the rapidity bin, $y = 0.45$ with a peak value of $v_1(0.45) = 0.177$. This was taken to be 100%. By decreasing the cell size to $dx = 0.35$ fm the peak value increased to $v_1(0.45) = 0.200$, i.e. by 13%. The changes of the directed flow peak values are shown in Table I.

TABLE I. Change of Directed Flow

y		Pb+Pb	Pb+Pb	Pb+Pb	Pb+Pb
	b/b_{max}	0.5	0.5	0.7	0.7
	dx, dy, dz [fm]	0.585	0.350	0.585	0.350
0.35	$v_1(y)$ [%]	-3	10	25	47
0.45	$v_1(y)$ [%]		13	32	53
0.55	$v_1(y)$ [%]	-3	9	20	50

For $b = 0.5b_{\text{max}}$ the KH instability on the v_1 -peak is weak, 13%, which can partly be attributed to the decreased viscous dissipation. At $b = 0.7b_{\text{max}}$, the increase is 21%, it is significantly stronger. These primary data of course are reduced by random initial state dissipation, as discussed in ref. [6]. The position of the peak in rapidity is hardly changing with higher grid resolution, for $b = 0.5b_{\text{max}}$ it moves from $y = 0.485$ to $y = 0.46$, while for $b = 0.7b_{\text{max}}$ it moves from $y = 0.475$ to $y = 0.46$.

Recently it was pointed out [15] that due to random initial fluctuations turbulence may show up and even grow

in the transverse, $[x, y]$ plane. The energy of the growth is provided by absorbing small, higher wave number perturbations. We also observed this effect (see Fig. 1). In that work an alternative detection method is suggested via measuring two particle correlations, which may also be used to detect the KH instability in the reaction plane.

Although, the predicted rotation effect is not easily detectable due to initial state fluctuations, the KH instability enhances the flow and changes its pattern in peripheral collisions. The present developments suggest that the global collective v_1 flow can be disentangled from random fluctuations. This is necessary to measure the global collective flow in peripheral collisions. The opposite, the separation of the flow originating from random initial state fluctuations is done successfully recently [16] for selected central collisions.

The KH instability is very sensitive to the magnitude of the viscosity. Thus if this research is successful the analysis of global collective v_1 flow as a function of beam energy and impact parameter may provide a precision measurement of viscosity and its variation.

Acknowledgements

We thank Martin Greiner, Peter Van and Pawel J. Kosinski for valuable discussions. L.P. Csernai and D.D. Strottman thank for the hospitality of Dirk Rischke, of the Frankfurt Institute for Advanced Studies and of the Alexander von Humboldt Foundation.

-
- [1] K. Aamodt et al., (ALICE Collaboration) Phys. Rev. Lett. 105, 252302 (2010).
 - [2] P.K. Kovtun, D.T. Son and A.O. Starinets, Phys. Rev. Lett. 94, 111601 (2005).
 - [3] L.P. Csernai, J.I. Kapusta, L.D. McLerran, Phys. Rev. Lett. 97, 152303-4 (2006).
 - [4] L.P. Csernai, and J.I. Kapusta, Phys. Rev. Lett. **69**, 737 (1992); and L.P. Csernai, and J.I. Kapusta, Phys. Rev. D **46**, 1379 (1992).
 - [5] L.P. Csernai, Y. Cheng, V.K. Magas, I.N. Mishustin, and D. Strottman, Nucl. Phys. A 834, 261c (2010).
 - [6] L.P. Csernai, V.K. Magas, H. Stöcker, and D.D. Strottman, Phys. Rev. C 84, 02914 (2011).
 - [7] V.K. Magas, L.P. Csernai, and D.D. Strottman, Phys. Rev. C 64 (2001) 014901; and V.K. Magas, L.P. Csernai, and D. Strottman, Nucl. Phys. A 712 (2002) 167.
 - [8] Drazin P.: Introduction to Hydrodynamic Stability (CUP, 2002)
 - [9] A. N. Kolmogorov, Proc. of the USSR Academy of Sciences 30, 299-303 (1941).
 - [10] Sz. Horvat, V.K. Magas, D.D. Strottman, L.P. Csernai, Phys. Lett. B 692, 277 (2010).
 - [11] H.J. Warringa, A. Sedrakian, Phys. Rev. A **84**, 023609 (2011); M. W. Zwiernie, J. R. Abo-Shaeer, A. Schirotzek, C. H. Schunck, and W. Ketterle, Nature (London) 435, 1047 (2005).
 - [12] L.D. Landau and E.M. Lifshitz: Hydrodynamics (Vol. VI) Nauka, Moscow (1953)
 - [13] P.A. Davidson: Turbulence, Cambridge University Press (2004)
 - [14] Krasny, R. J. Comp. Phys. 65, 292-313 (1986).
 - [15] S. Floerchinger, U.A. Wiedemann, JHEP 11, 100 (2011).
 - [16] K. Aamodt et al., (ALICE Collaboration) arXiv:1105.3865v1 [nucl-ex], and CERN Courier, October 2011, p. 6